The interfacial slippage of paper during blade metering

P. Alam *and* ***M. Toivakka***

Laboratory of paper Coating and Converting, Faculty of Chemical Engineering, Åbo Akademi University, Porthaninkatu 3, 20500-FIN, Turku, Finland

Abstract

Numerical methods were used to model fluid-solid interactions during blade metering applications. Paper attached to an elastomeric backing roll was used to drive Newtonian coating colours up to speeds of $20ms^{-1}$ under either steel or composite polymeric-steel metering blades. Parameters such as the coating viscosity, coating thickness and paper web speed were all found to influence the magnitude of paper slip and separation at the backing roll interface. The use of thin steel blades was found to lessen separation of paper relative to the thicker composite polymeric-steel blades and this is related to the increased slip as a function of distance leading to increased buckling. Interfacial slippage of paper from the backing roll is found to be linearly proportional to interfacial separation. In conclusion, the interfacial slip that occurs between the paper and the backing roll is related to an amalgamation of events that primarily comprise the coating pressure under the blade, the value of the coefficient of static friction and the mechanical properties of the backing roll material. The interfacial slip and separation are thus also implicitly related to the coating properties such as the viscosity, thickness and velocity since this affects the magnitude of the pressure pulsation under the metering blade.

1 Introduction

Paper coatings are frequently subjected to an operation known as blade metering. In this operation, coating colours are driven by the paper web at high velocities underneath a metering blade and the coating colours are levelled to a desired coat weight. The operation can be effectively used to control and optimise factors such as the opacity, the printability and the mechanical properties. The most traditional material for the metering blade is steel, however, both ceramic-steel and polymeric-steel soft-tip blades have the potential of more frequently being used as they are more resistant to wear. During the metering process, local components, such as the metering blade the paper and the backing roll, deform and deflect as a result of the high pressure variations generated when the coating colours are compressed between them, [1]. This deformation of paper and backing roll materials has been modelled using finite element methods [2] and strain profiles were generated from these models for the backing roll materials. The models, however, utilised a very low elastic modulus value for the backing roll material (5MPa). Higher elastic modulus values of 0.15GPa were applied in blade metering models that included backing roll deformation [3]. Experimentally based reports on the storage modulus of viscoelastic composite backing roll [4] range values between 2.65-2.75GPa for high frequency loading operations (1-25Hz respectively). Since the elastic properties of viscoelastic materials are wholly compatible with their strain rate, the use of higher modulus values may be better suited to high velocity metering applications. Interfacial strain differentials that arise between the paper and the backing roll can result in interfacial slippage between the materials leading to paper-backing roll separation. The research presented in this paper takes modelling of the deformation characteristics observed in blade metering operations a step further by studying the phenomenon of interfacial slip and separation between paper and the backing roll.

2 Methodological approach to modelling

Multiphysics simulations were initially carried out using FEMLAB finite element software and data was subsequently transferred to ANSYS finite element software for the analysis of interfacial slip. Composite polymeric-steel blades as well as traditional steel blades were modelled together with the coating colour, the base paper substrate and the elastomeric baking roll material. The discretised geometries used in the analyses can be seen in Figure 1.

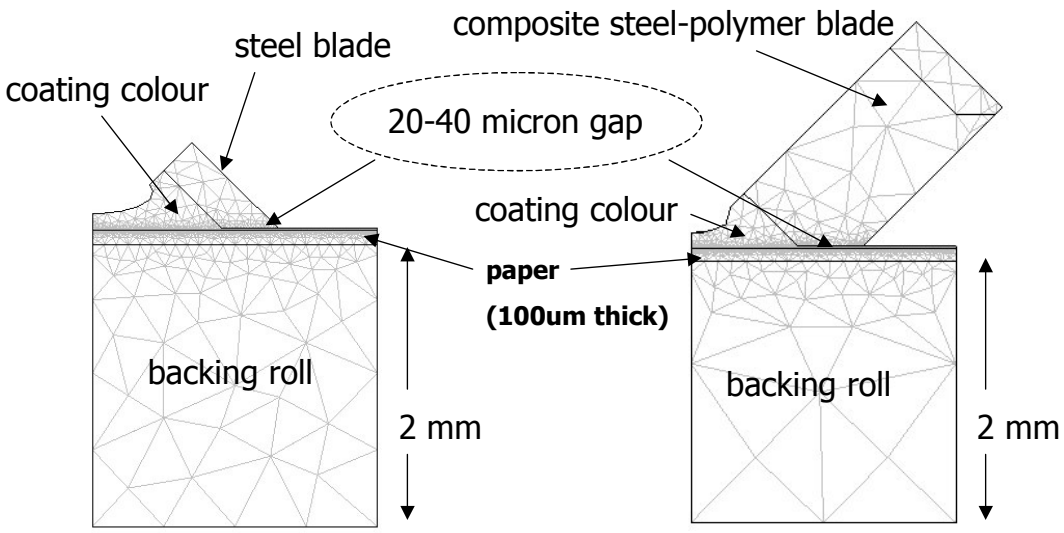

Figure 1. Discretised geometries for comparative steel blade and soft-tip blade models.

A moving boundary was applied to the surface of the base paper substrate in contact with the coating colour and thereby became sole the driving force for coating colour flow under the blade tip. This moving boundary was applied as a means of mimicking the paper web velocity. The coatings colours followed Navier-Stokes equations for incompressible Newtonian flow, Equations 1 and 2.

$$\rho\frac{\partial u}{\partial t}-\eta\nabla^2 u+\rho(u\cdot\nabla)u+\nabla p=F \qquad (1)$$

$$\nabla\cdot u=0 \qquad (2)$$

where

- η is the dynamic viscosity
- ρ is the density
- u is the velocity field
- p is the pressure
- F is a volume force field

Coating colours were simulated at viscosities ranging between 20-80mPas, however, these viscosities were non-linearly factored [5] to account for the increase in the coating solids content that arises underneath the blade due to conjoint pressure and dewatering effects. For example 20, 40, 60 and 80mPas would be factored to 20, 389, 998 and 1606mPas respectively, which are more accurate viscosity values for coating colours under the blade. The density of the coating was kept at a constant value of 1400kgm^{-3} throughout the simulations.

High velocity coating flow between the paper and the blade tip inevitably deforms the blade, the paper and backing roll materials. Since the analysis was two-dimensional, these solid components were subsequently defined and would deform as plane stress materials. At high strain rates, viscoelastic materials exhibit Hookean behaviour whereas at lower strain rates viscous characteristics predominate. Since the rate of material straining is phenomenally high

during the metering operation (~ 40kHz), the viscoelastic paper and backing roll materials also followed the constitutive equations for Hookean elastic solids. The isotropic materials (steel, polymeric soft-tip and elastomeric backing roll) thus followed the form of Equation 3, whilst the base paper substrate, approximated to an orthotropic solid, followed the form of Equation 4.

$$\varepsilon = \frac{\sigma}{E} \quad (3)$$

$$\begin{bmatrix} \varepsilon_1 \\ \varepsilon_2 \\ \gamma_{12} \end{bmatrix} = \begin{bmatrix} \frac{1}{E_1} & -\frac{\nu_{21}}{E_2} & 0 \\ -\frac{\nu_{12}}{E_1} & \frac{1}{E_2} & 0 \\ 0 & 0 & \frac{1}{G_{12}} \end{bmatrix} \cdot \begin{bmatrix} \sigma_1 \\ \sigma_2 \\ \tau_{12} \end{bmatrix} \quad (4)$$

where

- ε is the normal strain
- σ is the normal stress
- γ is the shear strain
- τ is the shear stress
- υ is the Poisson's ratio
- E is the elastic modulus

The properties input for the steel were E = 210GPa and υ = 0.33. For the polymeric soft-tip, the properties were applied as E = 1.1GPa and υ = 0.3. The elastomeric backing roll was given properties that were taken from the literature [4] where E = 2.75GPa and υ = 0.499. Literature values for the paper [6] were used yielding the values; $E_1 = E_{MD}$ = 7.44GPa, $E_2 = E_z$ = 39MPa, $\upsilon_{12} = \upsilon_{21}$ = 0.021 and G_{12} = 0.099GPa. For paper the subscript $_{MD}$ refers to the machine direction and the subscript $_z$ refers to the thickness direction.

Force transfer from the coating colour to the solid material components is achieved using Equations 5-8, which are set at the fluid-to-solid interfacial boundaries using MATLAB expressions and describe the total force per unit area, F^T.

$$F_{x_i}^T = \left\{ -\sum_j n_j \left[-p\delta_{ij} + \eta \left(\frac{\partial u_i}{\partial x_j} + \frac{\partial u_j}{\partial x_i} \right) \right] \right\} \quad (5)$$

$$F_{y_i}^T = \left\{ -\sum_j n_j \left[-p\delta_{ij} + \eta \left(\frac{\partial v_i}{\partial y_j} + \frac{\partial v_j}{\partial y_i} \right) \right] \right\} \quad (6)$$

$$F_{x_j}^T = \left\{ -\sum_i n_i \left[-p\delta_{ji} + \eta \left(\frac{\partial u_j}{\partial x_i} + \frac{\partial u_i}{\partial x_j} \right) \right] \right\} \quad (7)$$

$$F_{y_j}^T = \left\{ -\sum_i n_i \left[-p\delta_{ji} + \eta \left(\frac{\partial v_j}{\partial y_i} + \frac{\partial v_i}{\partial y_j} \right) \right] \right\} \quad (8)$$

where

- u and v are directional velocities
- x and y are directional components
- δ is a scaling coefficient
- n is an outward normal vector

The deformed solid components result in an increased coating cross-section, which alleviates pressure in the coating. The reduced pressure in the coating gives rise to strain relaxation in the solids thereby decreasing the coating cross-section and increasing the pressure. This cyclically orienting behaviour eventually reaches equilibrium and the equilibrium pressures calculated by the model are acquired by parametrically solving the coating flow as incremental functions of the coating velocity, storing the solutions and subsequently parametrically solving the deformation characteristics as incremental functions of the calculated pressure profiles. The deformation solutions are then stored and the model solved for both pressures and deformation simultaneously from the stored solutions. In total, fifty-nine separate re-calculations are simulated to reach a credible state of equilibrium between the coating pressures and the deformations in each model.

To calculate the slip and separation of the paper from the backing roll, pressures from the FEMLAB models were then transferred to models developed using ANSYS software. This software proved more convenient for analysing solid-to-solid interfacial behaviour and the models were developed with a resistance function to interfacial slip by means of an equivalent shear stress defined in the Coulomb friction model, τ, which is influenced by the coefficient of static friction, μ_s. With this model, Equation 9, sliding begins as a fraction of the contact pressures and as symmetric solvers can be easily used with a linear model such as the Coulomb model, there are reduced convergence difficulties. Since the strain rate is high and the dwell time extremely short under the blade, the static coefficient of friction is believed to be sufficient for this analysis.

$$\tau = \mu_s p + c_h \quad (9)$$

where

- τ is the contact shear stress
- p is the pressure calculated by the model
- μ_s is the coefficient of static friction
- c_h is the force of cohesion (given a value of zero)

The pressures generated on the surface of the paper were transferred using a FORTRAN algorithm, which averaged pressures as a function of the distance across each element edge and is described in Equation 10.

$$\bar{p} = \frac{1}{n_i} \sum_i p_i \quad (10)$$

where

- $\bar{p}$ is the mean pressure value calculated for each element edge
- n_i is an integer equal to the number of p_i summated
- p is the output pressure

4 Effects of blade type

Traditional steel blades are compared in this section with polymeric-steel soft-tip blades with regard to their influence on slip and separation at the paper-backing roll interface. The coating thickness under the blade was studied for 40µm coating layers and run at paper web velocities of 5, 10, 15 and 20ms^{-1}. The coefficient of static friction was given a constant value of 0.1.

At equilibrium, the pressures are relatively similar for both steel and polymeric soft-tip blades, Figure 2. Yet, there is clearly more interfacial slip occurring for the soft-tip metering blades, Figures 3 and 4. Furthermore, as the magnitude of slip increases, so too does the separation at the interface before and after the metering blade, Figures 5-8. The explanation can be aided by pictographically visualising the situation, refer to Figure 9. Slip progresses from a neutral slip point under the blade reaching the highest magnitude of slip at the outlet of the blade. The slip and separation is considerably lower at the inlet than at the outlet of the blade. This phenomenon is quite plausibly due to increased constraint of paper movement from the presence of high localised pressures that develop at the blade inlet, Figure 10. The lateral slip movement pushes the paper along the machine direction and causes it to buckle due to geometric instabilities, which gives rise to interfacial separation.

Since the effective length of the metering blade tip is longer for the soft-tip blade, the magnitude of slip is higher than in the steel blade and the extent of buckling is thence higher.

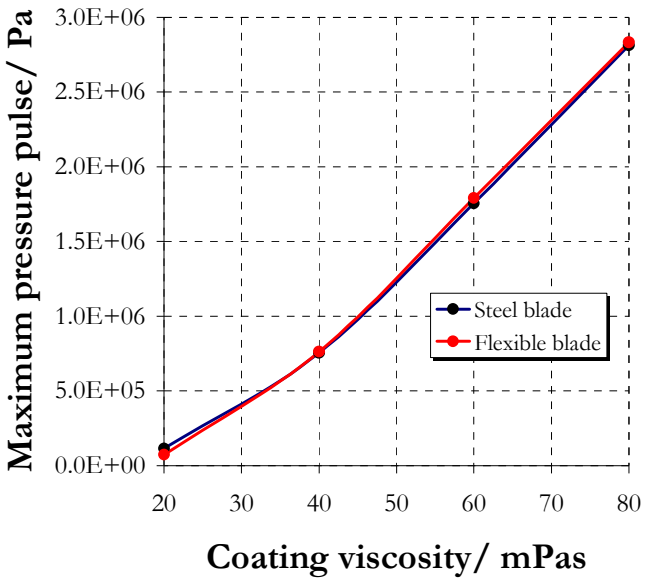

Figure 2. Maximum equilibrium pressure pulse as a function of the coating viscosity at a velocity of 20ms^{-1} for both steel and soft-tip blades.

Interfacial slip and interfacial separation before the blade can be easily identified to be a power law function of the coating viscosity. This is the logical outcome since the viscosities are non-linearly factored according to [5] as the solids content of the coating colour increases significantly under the blade as the coating viscosity heightens. The separations after the blade seem to be linearly proportional to the viscosity at the lower paper web velocities, though, at higher velocities the same power law trend becomes increasingly apparent.

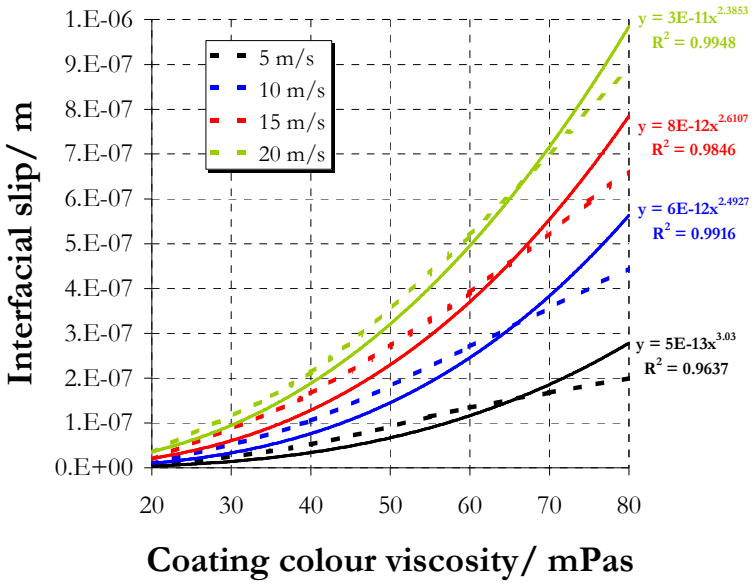

Figure 3. Interfacial slip as a function of the coating colour viscosity at different paper web velocities for soft-tip blades.

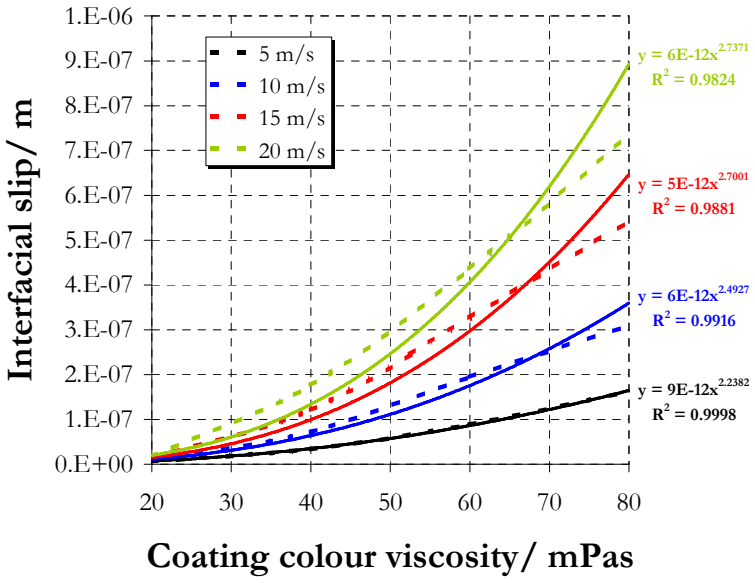

Figure 4. Interfacial slip as a function of the coating colour viscosity at different paper web velocities for steel blades.

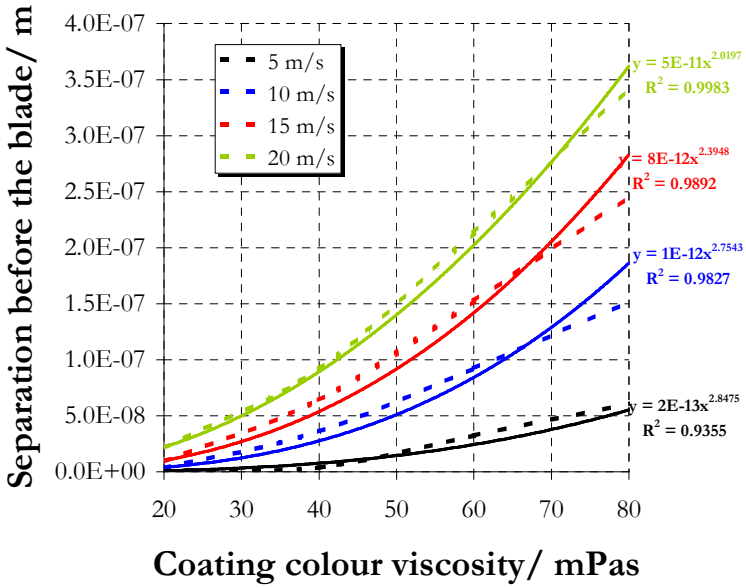

Figure 5. Separation before the blade as a function of the coating colour viscosity at different paper web velocities for soft-tip blades.

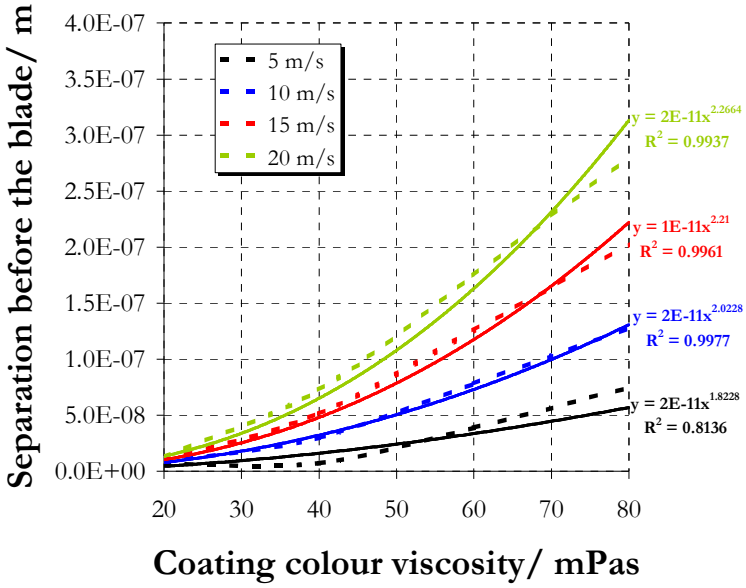

Figure 6. Separation before the blade as a function of the coating colour viscosity at different paper web velocities for steel blades.

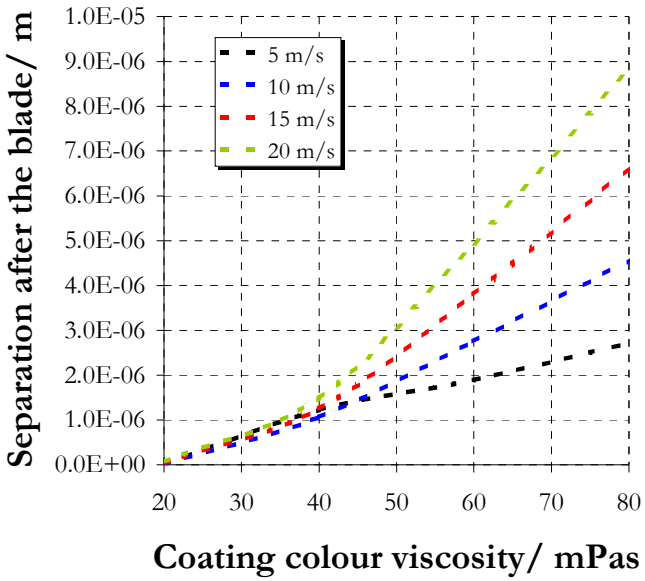

Figure 7. Separation after the blade as a function of the coating colour viscosity at different paper web velocities for soft-tip blades.

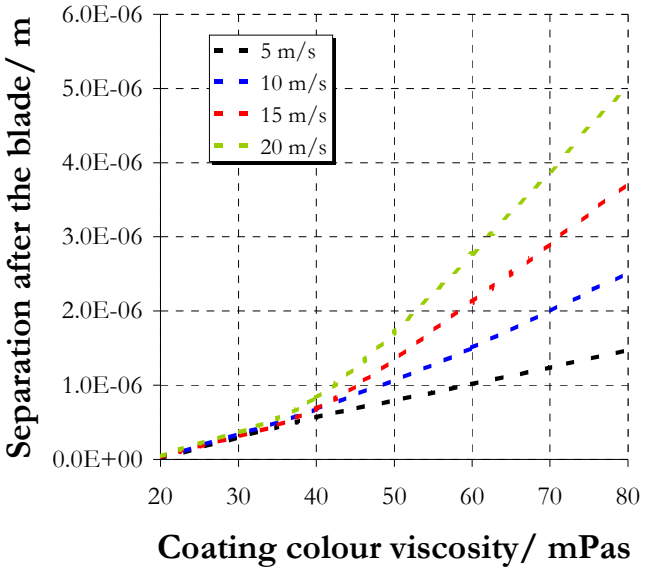

Figure 8. Separation after the blade as a function of the coating colour viscosity at different paper web velocities for steel blades.

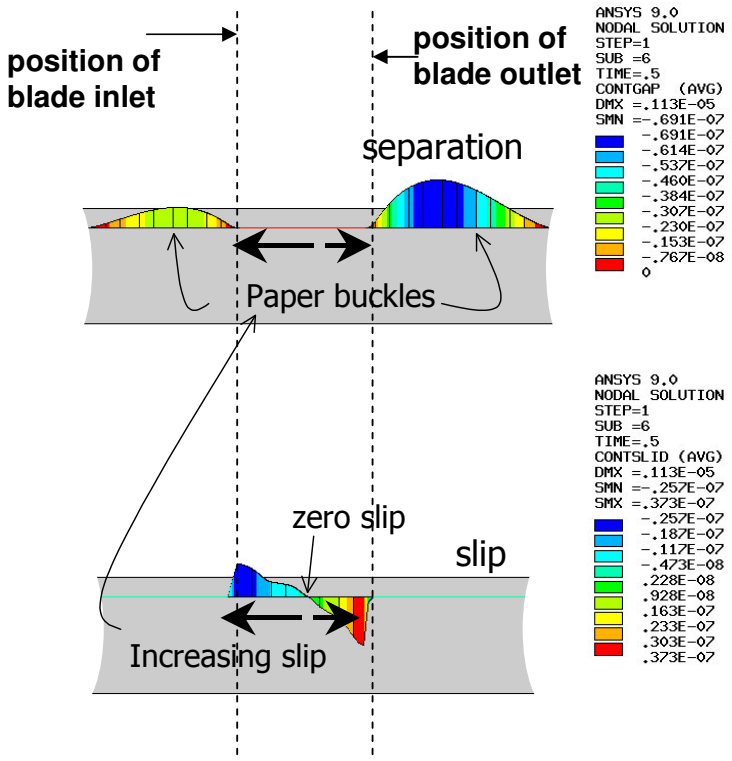

Figure 9. Example of separation and slip where paper slips form the backing roll towards the inlet and outlet ends of the blade tip. The force generated from this slippage pushes and buckles the paper at the blade tip ends resulting in interfacial separation.

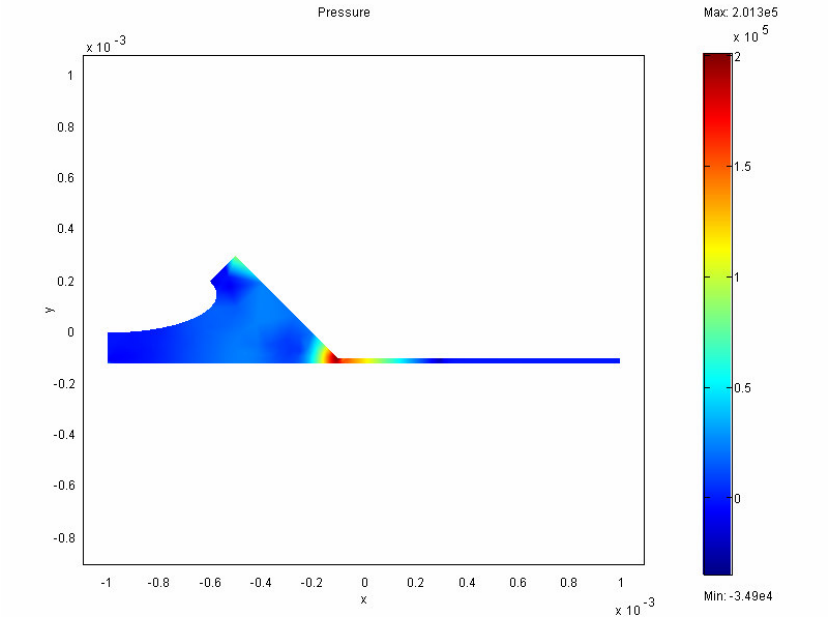

Figure 10. Example of the high pressure that develops in the coating at the blade inlet. This is conceivably the reason that slip and separation at the paper-backing roll interface is lower at the blade inlet than at the outlet.

When the maximum values of slip are plotted as a function of the maximum values of separation before and after the blade ends, linear proportionality is found to exist between the two for both blade types, Figures 11-14. The regression is further reinforced by the high determination coefficients. It is conceivable that this linear relationship would cease to exist on reaching at least the fracture strain of the base paper material. At this point, the paper web would separate and the ambient pressure would generate a more radical buckle before and after the blade.

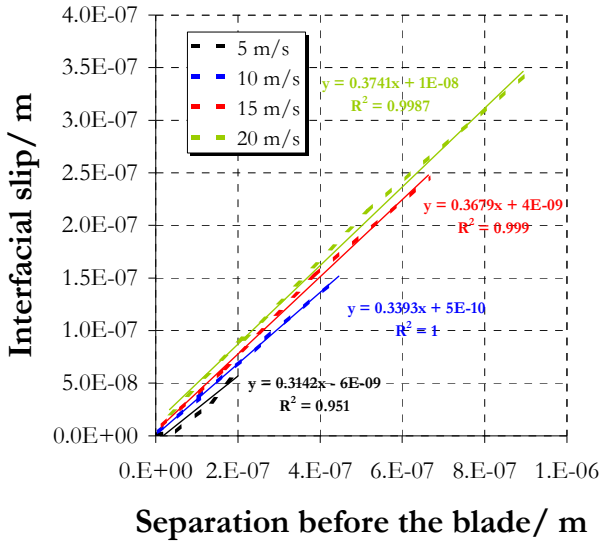

Figure 11. Interfacial slip plotted as a function of interfacial separation before the blade inlet shows linear proportionality for the soft-tip blades.

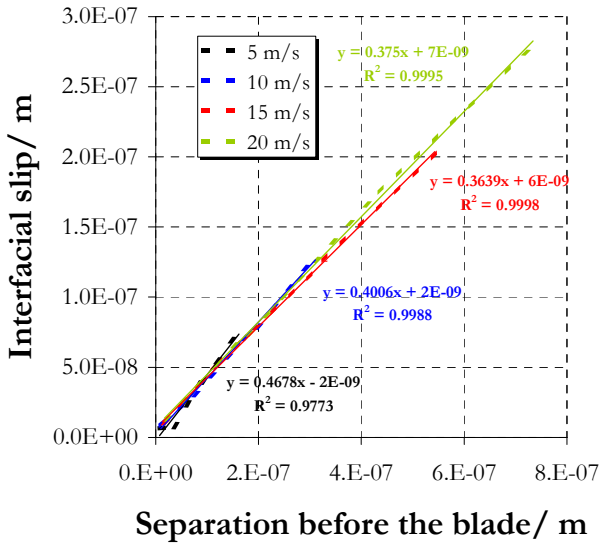

Figure 12. Interfacial slip plotted as a function of interfacial separation before the blade inlet shows linear proportionality for the steel blades.

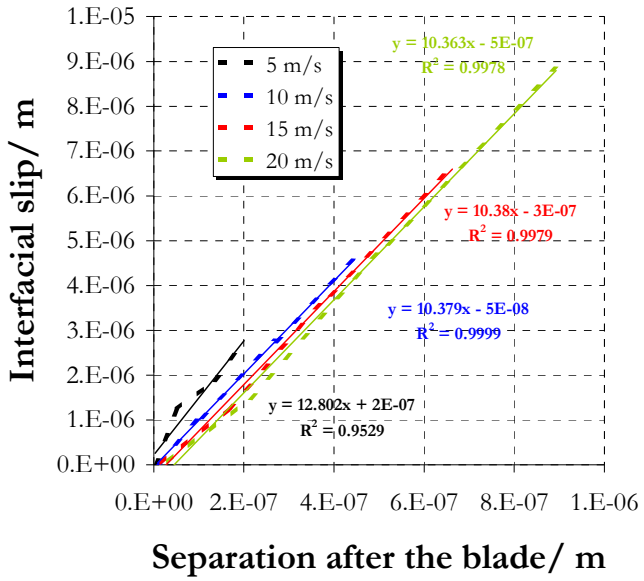

Figure 13. Interfacial slip plotted as a function of interfacial separation after the blade inlet shows linear proportionality for the soft-tip blades.

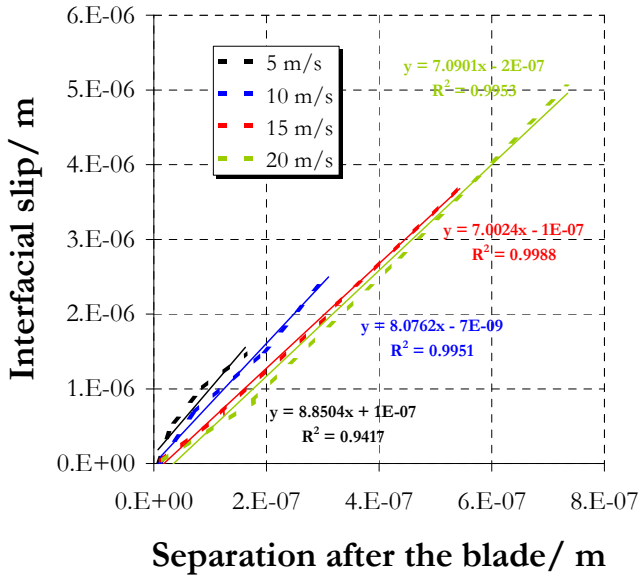

Figure 14. Interfacial slip plotted as a function of interfacial separation after the blade inlet shows linear proportionality for the steel blades.

5 Effects of the coating thickness

In this section, the coating thickness effects on the slip-separation characteristics are investigated for soft-tip blades. The coating thickness is defined as the original distance between the paper and the bottom of the blade. Figures 15 and 16 show the interfacial slip and separation before the blade inlet plotted as a function of increasing coating thickness. The paper web

velocity was 20ms^{-1} and the coefficient of static friction set at 0.1. The simulations were carried out using viscosities of 20, 40, 60 and 80mPas and in every case, the interfacial slip or separation decreases as a function of an increasing coating thickness. As the coating thickness is increased, the area increases proportionally and the pressure is reduced. The effect of viscosity was consistently non-linear, and is due to the increased solids content under the blade [5].

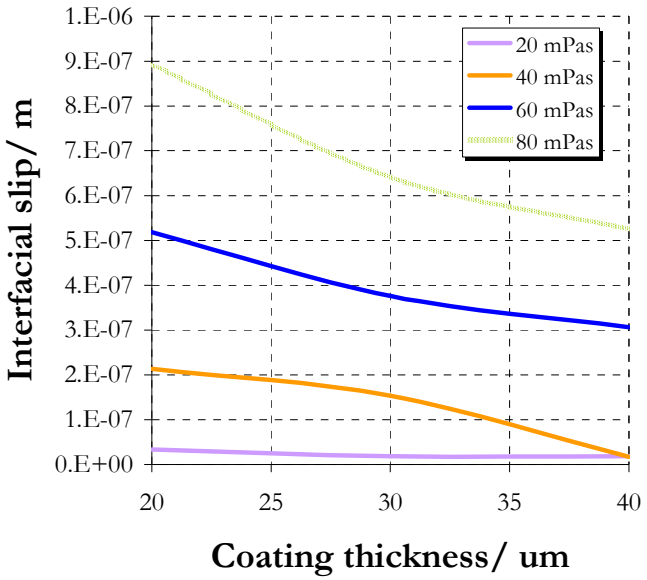

Figure 15. Interfacial slip plotted as a function of increasing coating thickness using coatings of different viscosities.

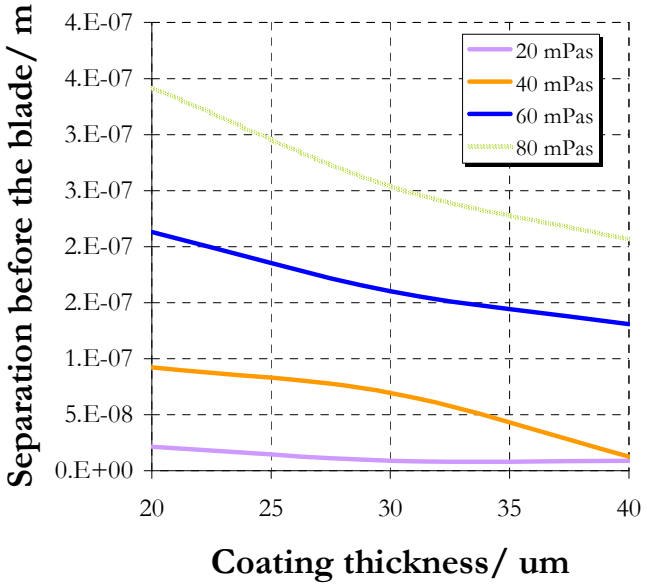

Figure 16. Separation before the blade plotted as a function of increasing coating thickness using coatings of different viscosities.

6 Effects of friction

The effect of the coefficient of static friction is studied in this section as an independent variable for soft-tip blade models. Three friction coefficients were used, 0.1, 0.5 and 0.9, with a coating thickness of 20µm and a paper web velocity of 20ms^{-1}. The slip and separation at the interface were found to be influenced by the static friction coefficient with the higher coefficients resulting in reduced slip and separation. Inverse linear proportionality is seen to exist between the slip-separation characteristic as a function of an increasing coefficient of static friction and high determination coefficients support this principle, Figure 17.

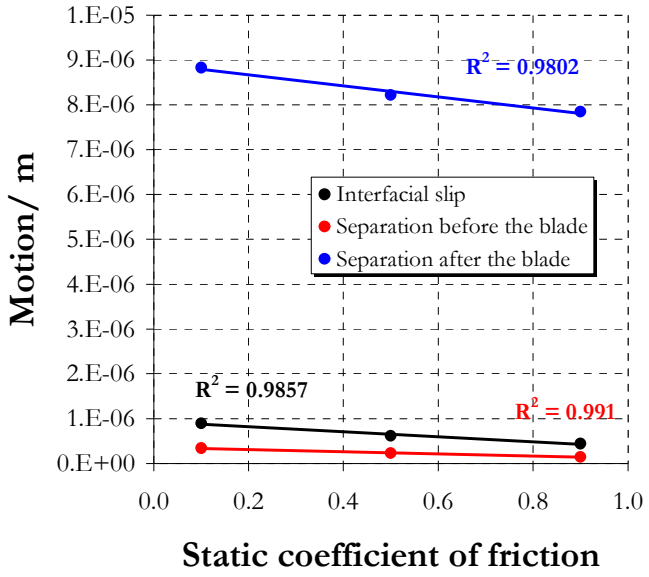

Figure 17. Slip-separation characteristics plotted as a function of the coefficient of static friction.

7 Effects of varying the backing roll properties

So far, the backing roll properties have invariably remained unchanged. This section studies the effects that arise from altering the elastic modulus of the backing roll material during soft-tip blade metering. Numerous backing roll elastic modulus values were used ranging from 0.005GPa (as modelled in [2]) to just over 7GPa. A static friction coefficient of 0.1 was used, a coating thickness of 20µm, a coating viscosity of 80mPas and a paper web velocity of 20ms^{-1}.

Figure 18 shows the maximum separation distance plotted as a function of increasing backing roll stiffness. The relationship is evidently non-linear and the magnitude of separation lessens dramatically as the stiffness of the backing roll is decreased. The separation begins to plateau beyond a stiffness of approximately 3GPa and the use of harder materials makes little difference to the magnitude of slip.

It can be hypothesised that a higher extent of backing roll deformation transpires when using lower stiffness backing roll materials, which in turn decreases paper buckling since the paper encounters lessened mechanical resistance and more readily deforms than slips. As the stiffness of the backing roll is increased, the deformation decreases and residual energy is released by paper buckling. The plateau is in effect an indication of consistently low backing roll deformations where similar amounts of residual energy are released through the mechanism of

paper buckling. As lifting paper can pose problems during metering operations, the use of lower stiffness backing roll material might be considered a means to design optimisation.

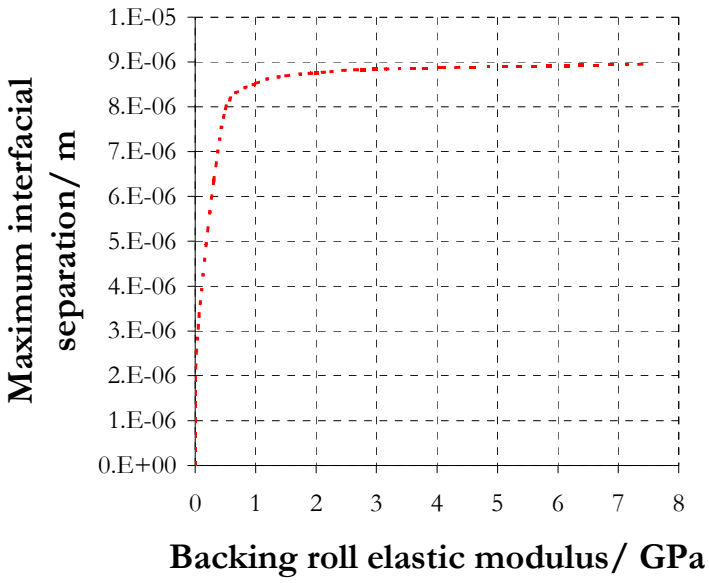

Figure 18. Maximum interfacial separation plotted as a function of the backing roll elastic modulus.

8 Conclusions

- Interfacial slippage of paper causes paper separation by buckling the paper in a geometrically unstable machine direction.
- Slip and separation is significantly lower at the blade inlet than at the blade outlet, most conceivably because the blade inlet experiences a slip constraining pressure pulsation.
- Interfacial slippage of paper from the backing roll is linearly proportional to interfacial separation of paper from the backing roll.
- Thicker blades augment the slip and separation of paper from the backing roll because higher machine direction deformations result in larger machine direction buckles.
- Increasing the coating viscosity and/ or the paper web speed increases the magnitude of pressure experienced under the blade and results in higher slip and separation characteristics.
- Increasing the coating thickness lowers the pressure under the blade and reduces the slip-separation characteristics.
- Interfacial slip and separation are inversely proportional to the coefficient of static friction.
- Lowering the elastic modulus of the backing roll material may alleviate the problems associated with interfacial slippage and separation of paper from the backing roll.

9 Ackowledgments

The authors would like to thank Jorma Kinnunen, Metso Paper Inc. Wärtsilänkatu 100 FI-04400, Järvenpää, Finland, for his practical advice in this research.

10 References

1. Linnonmaa, J. and Trefz, M., 2000, Pigment coating techniques, *Pigment coating and surface sizing of paper*, Editor Lehtinen, E, Papermaking Science and Technology.
2. Bousfield, D. W., Wikstrom, M. and Rigdahl, M., 1998, Roll deformation during blade coating, Tappi Journal, **8(5)**, 207-212.
3. Pajari, H. Mansikka-ajo, J., Ketoja, J. and Bousfield, D. W., 2003, Blade coating with free jet applicator: modelling and experiments, *8th Advanced Fundamentals Symposium*, Chicago, IL, USA.
4. Vuoristo, T., Kuokkala, V. T. and Keskinen, E., 2000, Dynamic compression testing of particle-reinforced polymer roll cover materials, Composites: Part A, **31**, 815-822.
5. Eklund, D., Grankvist, T. O. and Salahetdin, R., 2003, The influence of viscosity and water retention on blade forces, *21st PTS Coating Symposium*, München, Germany.
6. Mann, R. W., Baum, G. A. and Habeger, C. C., 1980, Determination of all nine orthotropic elastic constants for machine-made paper, Tappi, **63(2),** 163-166.